Article

Synthesis and Characterisation of Highly Active and Coke Resistant Ni/SBA-15 Catalysts for Dry Reforming of Methane

Saeed Hajimirzaee , Emmanuel Iro , Maria Olea *

Posted Date: 27 February 2025

doi: 10.20944/preprints202502.2123.v1

Keywords: Dry reforming of methane; Ni/SBA-15 catalysts preparation; electrostatic adsorption; nickel complexes; carbon deposition; catalyst stability; ultrafine nickel nano particles

Article

Synthesis and Characterization of Highly Active and Coke Resistant Ni/SBA-15 Catalysts for Dry Reforming of Methane

Saeed Hajimirzaee [1,2], Emmanuel Iro [1,3] and Maria Olea [1,*]

[1] School of Science, Engineering & Design, Teesside University, Middlesbrough, TS1 3BX, United Kingdom
[2] CLARIANT QATAR W.L.L, MESAIEED INDUSTRIAL CITY, Qatar, P.O.BOX : 50240
[3] UNICAT Catalysts Technologies, LLC, 5918 South Highway 35, Alvin, TX 77511, USA
* Correspondence: author: M.Olea@tees.ac.uk

Abstract: A series of newly-developed Ni/SBA-15 catalysts were synthesised by combining strong electrostatic adsorption (SEA) of $[Ni(En)_3]^{2+}$ (En = ethylenediamine), $[Ni(NH_3)_6]^{2+}$ and $[Ni(EDTA)]^{2-}$ complexes, respectively, and engineered SBA-15 support, or, in other words, by adopting Charge Enhanced Dry Impregnation (CEDI), to produce highly active catalysts with very small nickel particles, resistant to carbon deposition, sintering and deactivation phenomena associated with nickel based catalysts in dry reforming of methane (DRM). In parallel, other Ni/SBA-15 catalysts were prepared by conventional incipient wetness impregnation method with $[Ni(H_2O)_6]^{2+}$ complex and used as the reference catalysts. TEM, wide-angle XRD, EDX, TGA results and temperature programmed experiments confirmed that the catalyst's preparation method has a strong impact on the size of the generated nickel particles and the amount of Ni deposited, which in turn were responsible for the catalytic activity and coke resistance. SEA on SBA-15 deposits from 4.8 wt% to 6.1 wt% Ni, depending on the complex used, while the DI deposits only 3% wt of Ni. The size of resulting Ni particles is between 3 and 8 nm for the unwashed SEA samples. For the DI unwashed samples, the size is significantly bigger, at 20 – 50 nm. For the SEA washed samples before calcination, i.e., those synthesised by using $[Ni(NH_3)_6]^{2+}$ and $[Ni(En)_3]^{2+}$ complexes, the Ni particles size is less than 1 nm. For these catalyst's samples, only small amount of carbon was deposited during the DRM reaction as confirmed by TGA results at 0.08 and 0.13 %.

Keywords: dry reforming of methane; Ni/SBA-15 catalysts preparation; electrostatic adsorption; nickel complexes; carbon deposition; catalyst stability; ultrafine nickel nano particles

1. Introduction

Dry (CO_2) reforming of methane (DRM) is gaining increasing attention because two problematic greenhouse gases which are in abundance; methane (from natural gas production and landfill gas) and carbon dioxide (from several cheap sources of carbon) can be converted to syngas (H_2 and CO), a building block for production of liquid fuels, chemicals and electricity generation [1–8]. Biogas from either anaerobic decomposition or thermochemical conversion of biomass such as gasification and pyrolysis is also receiving attention as an alternative to natural gas for energy sustainability [9–13]. Hot biogas from gasification or pyrolysis of organic matter contains methane and CO_2 either in similar ratio or higher methane to CO_2 ratio, and so converting the gas to H_2 and CO with little or no CO_2 left in the product stream is seen as a way of increasing the gas calorific value [14,15].

Dry (CO_2) reforming of methane is a highly endothermic reaction and requires a stable catalyst that will not sinter and easily deactivate within the optimum reaction temperature region, usually 600 – 800 °C [16]. Catalysts containing noble group VIII metals such as Pt, Pd, Ru, Ir. etc. have been reported to be highly active in DRM, however their high cost and scarcity make them commercially unattractive for any scale-up process. Alternatively, cheap and relatively abundant non noble metals,

 doi:10.20944/preprints202502.2123.v1

especially nickel is most sort after as its catalytic activity is comparible to those of nobel metals in DRM, however, nickel based catalysts are easily prone to carbon deposition and consequently deactivation which is a major setback to its full scale commercial application [17–24]. For this reason, many researchers have tried to improve on the synthesis of more stable nickel based catalysts with longer catalyst life time in DRM, unfortunately, rapid coking and subsequent deactivation of nickel based catalysts still remains an unresolved issue, especially in gas streams with higher methane to carbon dioxide ratios operated at tempertures above 600 °C [4,23,25–31].

The major reactions that take place along side DRM are shown below[32]:

1. Dry (CO_2) reforming of methane (DRM)

$$CH_4 + CO_2 \rightleftharpoons 2CO + 2H_2 \quad (\Delta H_{298K} = +247 \text{ kJ mol}^{-1}) \tag{1}$$

2. Decomposition of methane to form solid carbon and hydrogen

$$CH_4 \rightleftharpoons C_{(s)} + 2H_2 \quad (\Delta H_{298K} = +75 \text{ kJ mol}^{-1}) \tag{2}$$

3. Reverse water gas shift reaction (RWGS) occurs simultaneously with DRM to reduce H_2 produced during DRM reaction so that H_2/CO ratio could become slightly <1 where CH_4/CO_2 ratio is 1

$$CO_2 + H_2 \rightleftharpoons CO + H_2O \quad (\Delta H_{298K} = +41.2 \text{ kJ mol}^{-1}) \tag{3}$$

The water formed in Eqn (3) can either react with methane (methane steam reforming, MSR) as shown below:

$$CH_4 + H_2O \rightleftharpoons CO + 3H_2 \quad (\Delta H_{298K} = +206 \text{ kJ mol}^{-1}) \tag{4}$$

or can oxidise $C_{(S)}$ and reduce or eliminate coke deposition on the surface of the catalyst

$$C_{(s)} + H_2O_{(g)} \rightleftharpoons CO + H_2 \quad (\Delta H_{298K} = +131.3 \text{ kJ mol}^{-1}) \tag{5}$$

Reverse Boudouard reaction (BR) which involves the disproportionation of CO to form solid carbon and CO_2 is also possible, however from themodynamic point of view, this exothermic reaction which also includes possible CO_2 disproportionation reactions are not favourable under the high reaction temperatures above 600 °C used in dry methane reforming, and so the formation of solid carbon or coking on the surface of the catalyst during DRM is mainly from Eqn (2), and has the tendency to deposit and grow as armorphous, filamentous or graphite type of carbon. It has been reported that when nickel particles are poorly attached to the support, detached nickel particles are usually present. The formed carbon from methane decomposition (Eqn 2) easily encapsulate detached nickel particles to form a shell-like carbon coating, causing rapid catalyst deactivation with time during DRM [33–41]. Carbon formation from methane decomposition is more where the ratio of CH_4 to CO_2 is greater than one and at higher reaction temperatures above 600 °C [42]; and so only the most stable nickel catalysts resistant to sintering and coking can remain active for a long time in high temperature DRM with higher CH_4/CO_2 ratio.

In summary, it has been suggested that coke formation on nickel based catalysts and other catalysts are sensitive to:

1. Acid - basic character of support [43] (higher basicity increases the acidic CO_2 adsorption on the basic catalyst to form oxygen species from CO_2 disproportionation that can oxidise formed carbon and prevent catalyst coking for DCM below 600 °C)
2. Metal-support interactions [43] (active supports can supply reactive oxygen to oxidise and remove carbon)
3. Metal-support attachment (strongly attached nickel on support prevents shell-like carbon coating as explained earlier)
4. Metal crystalline structure [44,45] (smaller metal particles are usually more active thereby aiding formed water to quickly react with carbon to prevent coking on the surface of the catalyst. It is

 doi:10.20944/preprints202502.2123.v1

also more difficult to have a large carbon coating on ultrafine nickel particle, thereby aiding the ease of carbon oxidation during DRM)

In order to make DRM commercially viable, there is the need to develop cheap, thermally stable nickel based catalysts with high catalytic activity and resistance to coking.

Ever since the discovery of the synthesis of highly ordered mesoporous silica materials with high specific surface area, large pore size and volume, starting with MCM-41 in 1992, and then SBA-15 with better hydrothermal stability in 1998 [46–49], there has been a growing interest to apply SBA-15 as catalyst support material. It has been reported that SBA-15 cylindrical pores are capable of confining the growth of metal nano-particles and restricting their mobility and aggregation to prevent sintering and thus improve catalyst stability [50–52]; however, research has also shown that at high reaction temperatures, the cylindrical pore channels do not adequately mitigate the mobility of nickel nano-particles as they migrate out of the mesoporous channels to the external SBA-15 surface, resulting to sintering and eventual catalyst deactivation [53], and so it is still necessary to improve on the strength of metal – support attachment. For this reason, an investigation was carried out with different nickel complexes such as $[Ni(NH_3)_6]^{2+}$, $[Ni(En)_3]^{2+}$ (En = ethylenediamine) and $[Ni(EDTA)]^{2-}$ (EDTA = Ethylenediaminetetraacetic acid) to study the possibility of generating very small nickel particles having stronger attachement to SBA-15 support by strong electrostatic adsorption impregnation method and comparing the catalysts those from the conventional impregnation method with $[Ni(H_2O)_6]^{2+}$ complex which usually produces nickel with poorer attachement to SBA-15 support. It is important to note that for nickel based catalysts on inert supports such as SBA-15 with no significant suppy of surface oxygen, supported metal particles are the only active sites and therefore solely responsible for catalytic activity [54]. The type of SBA-15 mesoporous silica with high hydrothermal stability reported in our previous publication was used as catalyst support for all the nickel catalysts [55]. Since SBA-15 is inert and has no significant free lattice oxygen to contribute to the reaction and has neither Bronsted acidity nor basicity, the prevention of coke deposition will greatly depend on strong metal – support attachement and generation of small nano-nickel particles that are well dispersed in the pores and the external surfaces of SBA-15 which can promote rapid carbon-water oxidation reaction (Eqn 5). In this research, the synthesised Ni/SBA-15 catalysts were characterised and tested in dry (CO_2) reforming of methane using higher methane to carbon dioxide ratio (2.7:1) to study their activity, stability and resistance to coking.

2. Experimental

2.1. Conventional Methods for Synthesis of Ni/SBA-15 Catalysts

Ni/SBA-15 catalysts are usually prepared by the traditional incipient-wetness impregnation method which involves dissolving nickel salts in water to form greenish $[Ni(H_2O)_6]^{2+}$ complex by stirring for some minutes at room temperature before introducing it SBA-15 in solution. The as-synthesised Ni/SBA-15 sample is rarely washed with water due to the poor interaction between $[Ni(H_2O)_6]^{2+}$ complex and SBA-15. Our analysis of washed as-synthesised samples revealed that the nickel complex was completely washed away from SBA-15. The unwashed as-synthesised sample is then filtered, dried and calcined between 400 – 800 °C to burn off the complex, leaving only nickel (II) oxide (NiO) on the surface of the catalyst. Usually, this results in Ni/SBA-15 catalysts with some large detached nickel particles from the support that are prone to coking. Two different Ni/SBA-15 catalysts were prepared by heating one sample at 90 °C for 4 hours during incipient wetness impregnation while stirring, and the other stirred at room temperature for 8 hours, without washing both as-synthesied samples, followed by filtration, air drying and calcination at 550 °C for 6hrs. The catalysts were labelled as Ni/SBA-15-H_2O at 90 °C, unwashed and Ni/SBA-15 -H_2O at RT, unwashed, respectively.

 doi:10.20944/preprints202502.2123.v1

2.2. Novel Methods for Synthesis of Ni/SBA-15 Catalysts

Novel methods were proposed to improve on the interaction of nickel complex with SBA-15 as a means of generating small NiO particles, strongly attached to the support for higher catalytic activity and resistance to coking. Five catalysts were synthesised by simply displacing the water molecules around $[Ni(H_2O)_6]^{2+}$ complex with ammonia (NH_3) from ammonium hydroxide, ethylenediamine (En) and Ethylenediaminetetraacetic acid (EDTA) respectively. Each sample was either washed with water or not, except for Ni/SBA-15 catalyst prepared with EDTA. We noticed that unlike the other catalysts, washing the Ni-EDTA-SBA-15 as-synthesised catalyst with water removed the entire nickel complex from SBA-15 support. The reason for this is that washing with water increased the pH of solution, causing the surface of SBA-15 which has low isoelectric point (2 – 4) to become negatively charged, and so repelled the negatively charged Ni-EDTA complex.

All samples were calcined at 550 °C while another as-synthesied samples of Ni/SBA-15 (H_2O at 90 °C, unwashed) and Ni/SBA-15 (EDTA unwashed) were calcined at 700 °C due to observed incomplete removal of the complex at 550 °C from H_2 TPR results.

2.3. Catalyst Characterisation

The seven Ni/SBA-15 catalysts were characterised using Scanning Electron Microscopy (SEM) Hitachi S-3400N to study the morphology of the catalysts. Energy Dispersive X-ray spectroscopy (EDX) was used to analyse the amount of nickel loading on support. Wide angle X-ray Diffraction spectroscopy (XRD) patterns using Siemens D500 diffractometer with CuK α radiation (1.54 Å), at tube voltage of 40 KV and 20 mA current with data collected over 2θ range from 10 ° to 80 ° confirmed the presence and particle size of nickel oxide nanoparticles on SBA-15. Transmission Electron Microscopy (TEM) carried out on a JEOL 2100F FEG operating at 200 kV with samples ultrasonicated and dispersed onto holey carbon grids for examination in TEM mode was used to study the dispersion and size of nickel oxide on SBA-15. Nitrogen adsorption – desorption results were obtained in Micrometrics Tristar II degassed at 350 °C for 2 hours. BET method was used to calculate the surface area. Pore size and volume were determined from BJH adsorption isotherm. Thermal gravimetric analysis (TGA) of Thorn Scientific Services was used to measure weight losses of spent catalysts after reaction to determine carbon deposition.

2.4. Catalytic Reactions

Hiden Analytical CATLAB – quadripole mass spectrometer micro-reactor system of fixed bed quartz tube (4mm i.d and 18.5 cm in length) was used for temperature programed reaction experiments of all catalysts which includes H_2 TPR with 30ml/min of 5% H_2 in Ar heated from room temperature to 850 °C at 20°/min ramp rate, and dry reforming of methane (DRM). For dry reforming of methane experiments, the catalysts were first reduced with 30ml/min flowrate of 5% H_2 in He at 850 °C, followed by passing 27ml/min flowrate of 5% CH_4 in He and 10ml/min flowrates of 5% CO_2 in Ar over 35mg of each catalyst from room temperature to 850 °C, increasing the ramp rate at 20 °/min to determine optimum conversion tempeatures in one set of experiments, and in another set, the same CH_4 and CO_2 flowrates were passed over 35mg of H_2 reduced catalysts at 800 °C for 360 minutes time on stream for each catalyst. Thermal gravimetric analysis (TGA) was done on spent catalysts (for 360 minutes time on stream) to determine carbon content via percentage weight loss in oxidative atmosphere from 24 – 1000 °C at 10°/min ramp rate using 10 – 15mg of spent catalyst.

The percentage conversion for 360 minutes time on stream catalysts for CO_2 and CH_4 were calculated as:

$$\% \text{ Conversion } = \frac{Initial\ reactant\ partial\ pressure - Final\ reactant\ partial\ pressure}{Initial\ reactant\ partial\ pressure} \text{ x } 100$$

Product formation was observed on-line with noticible increases in the partial pressure signals of hydrogen and carbon monoxide from start-off reaction temperatures with corresponding decrease in the reactant partial pressures.

 doi:10.20944/preprints202502.2123.v1

3. Results and Discussions

3.1. Scanning Electron Microscope (SEM) Images of Fresh Catalysts

SBA-15 with worm-like morphology was used to prepare all the catalysts [55]. After impregnation with nickel complexes, all the catalysts retained SBA-15 worm-like morphology with primary particle sizes of the catalysts (1.2 - 3.1µm lengths and 0.4 – 0.6 µm widths) remaining same with SBA-15 support. Ni/SBA-15 (H_2O RT, unwashed) appeared to be crushed in most areas, the reason for this could be the long stirring time (8 hours) used for impregnation, however, TEM results confirm that the inner cylindrical pore structures were not damaged.

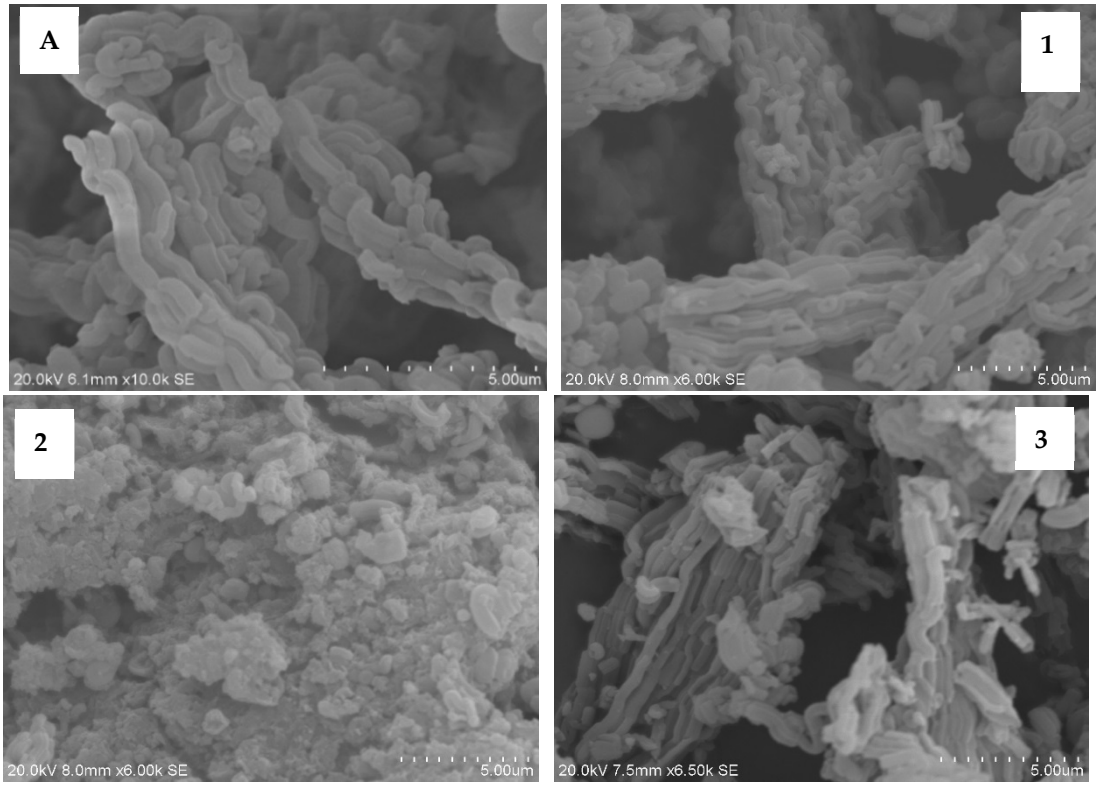

 doi:10.20944/preprints202502.2123.v1

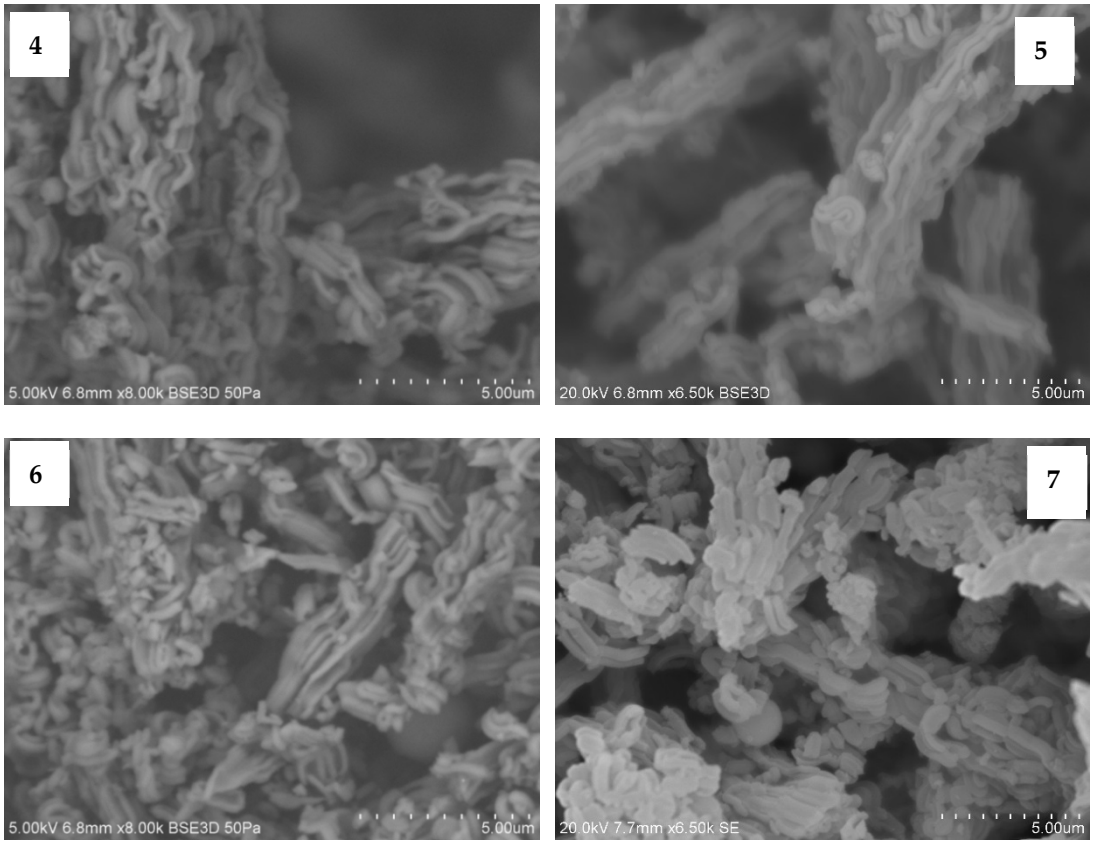

Figure 1. SEM images of pure SBA-15 support (A), Ni/SBA-15 – H_2O 90 °C, unwashed (1), Ni/SBA-15 H_2O at RT, unwashed (2), Ni/SBA-15 – En unwashed (3), Ni/SBA-15 – En washed (4), Ni/SBA-15 – NH_4OH unwashed (5), Ni/SBA-15 – NH_4OH washed (6), Ni/SBA-15 – EDTA unwashed (7).

3.2. Transmission Electron Microscope (TEM) Images

TEM of pure SBA-15 support viewed along x-y vertical plane (A) reveal the circular pores (5.4 nm diameter) surrounded by thick silica walls arranged in ordered 2D hexagonal fashion. When viewed along the x-y horizontal plane (B), the cylindrical pores with silica walls in-between are clearly seen. To maximise SBA-15 surface area for catalysis, impregnation or any other chosen method is usually aimed at generating and introducing very small metal particles inside the pore wall, as well as on the external surfaces. Ni/SBA-15 (H_2O at 90 °C, unwashed) catalyst show a well dispersed nickel loading on the surface of SBA-15 (1a – 1b). Ni/SBA-15 (H_2O at RT, unwashed) catalyst had large nickel particles that are poorly dispersed on SBA15 (2a – 2b). Ni/SBA-15 (En unwashed) catalyst had well dispersed nickel nano-particles on SBA-15; however, there are some bigger particles which appear detached from the SBA-15 support (3a – 3b). By washing the as-synthesised Ni/SBA-15 (En) sample with water, the bigger nickel particles loosely attached to the surface were washed off, leaving only ultrafine nickel particles on SBA-15 (4a – 4b), this explains why the Ni loading slightly dropped from 5.4 to 4.6 w/w % (Table 2), and also suggests that unlike Ni/SBA-15 (H_2O) catalysts, most of the nickel particles on Ni/SBA-15 (En unwashed) catalyst where strongly attached to the surface of SBA-15, and washing with water only removed the unattached nickel particles. With ammonium hydroxide, TEM images in 5a – 5b show that Ni/SBA-15 (NH_4OH unwashed) catalyst had both small and big Ni particles on SBA-15. Washing Ni/SBA-15- NH_4OH as-synthesised sample with water slightly reduced the Ni loading from 6.1 to 5.7 w/w % (Table 2), an indication that most of the nickel particles are strongly attached to SBA-15. Just like Ni/SBA-15 (En washed) catalyst, TEM image of Ni/SBA-15 (NH_4OH washed) catalyst reveal ultrafine, well dispersed and hardly visible Ni particles on SBA-15 (6a – 6b). Ni/SBA-15 (EDTA, unwashed) catalyst had well dispersed Ni particles with some slightly bigger particles on SBA-15 support shown in 7a – 7b,

 doi:10.20944/preprints202502.2123.v1

however sample was not washed with water as water quickly changed the pH of SBA-15, causing the complex to wash off due to like-charges with the support. It may be worthwhile to wash Ni/SBA-15 (EDTA) with solvent of pH less than 3, although this was not investigated further.

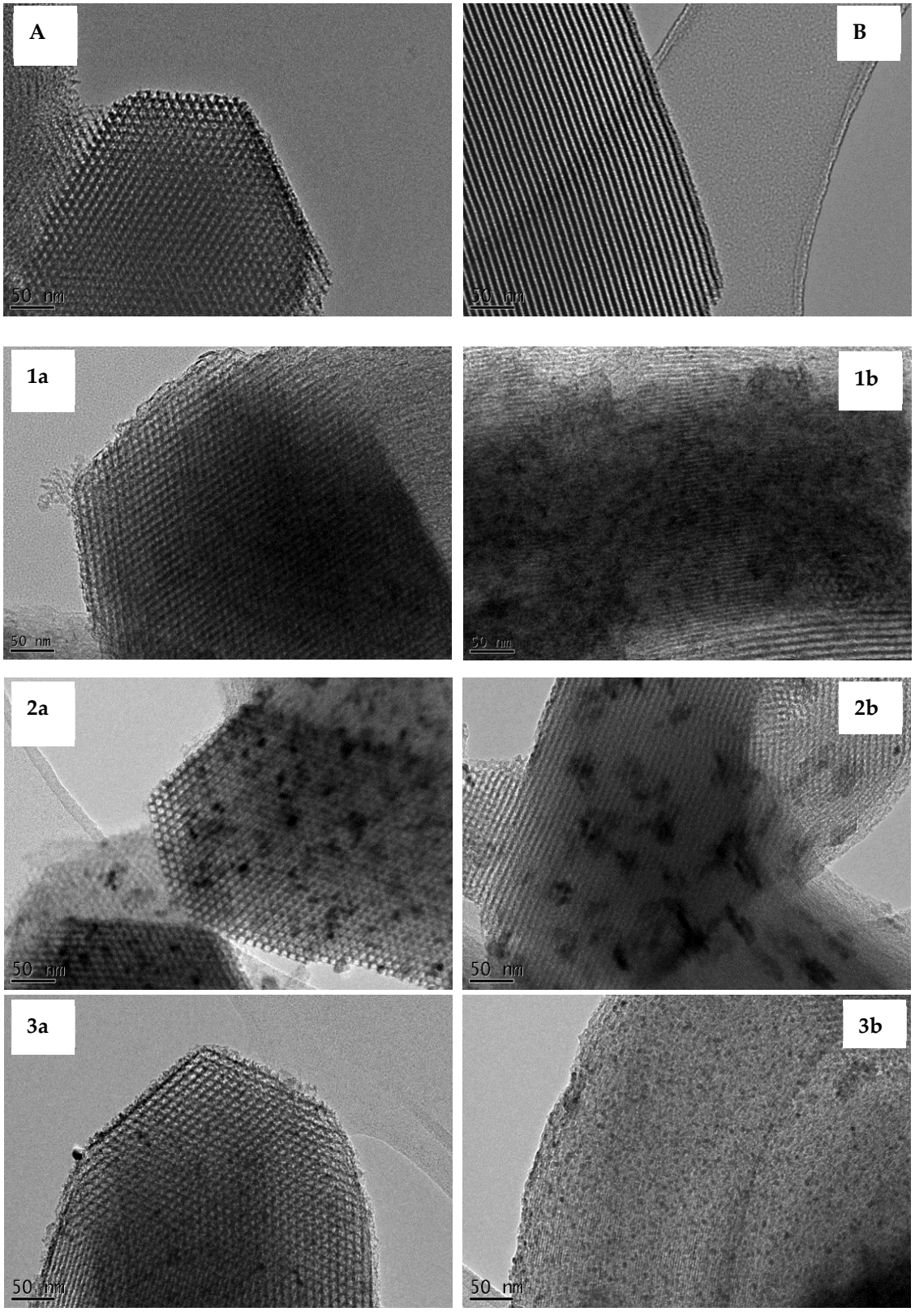

 doi:10.20944/preprints202502.2123.v1

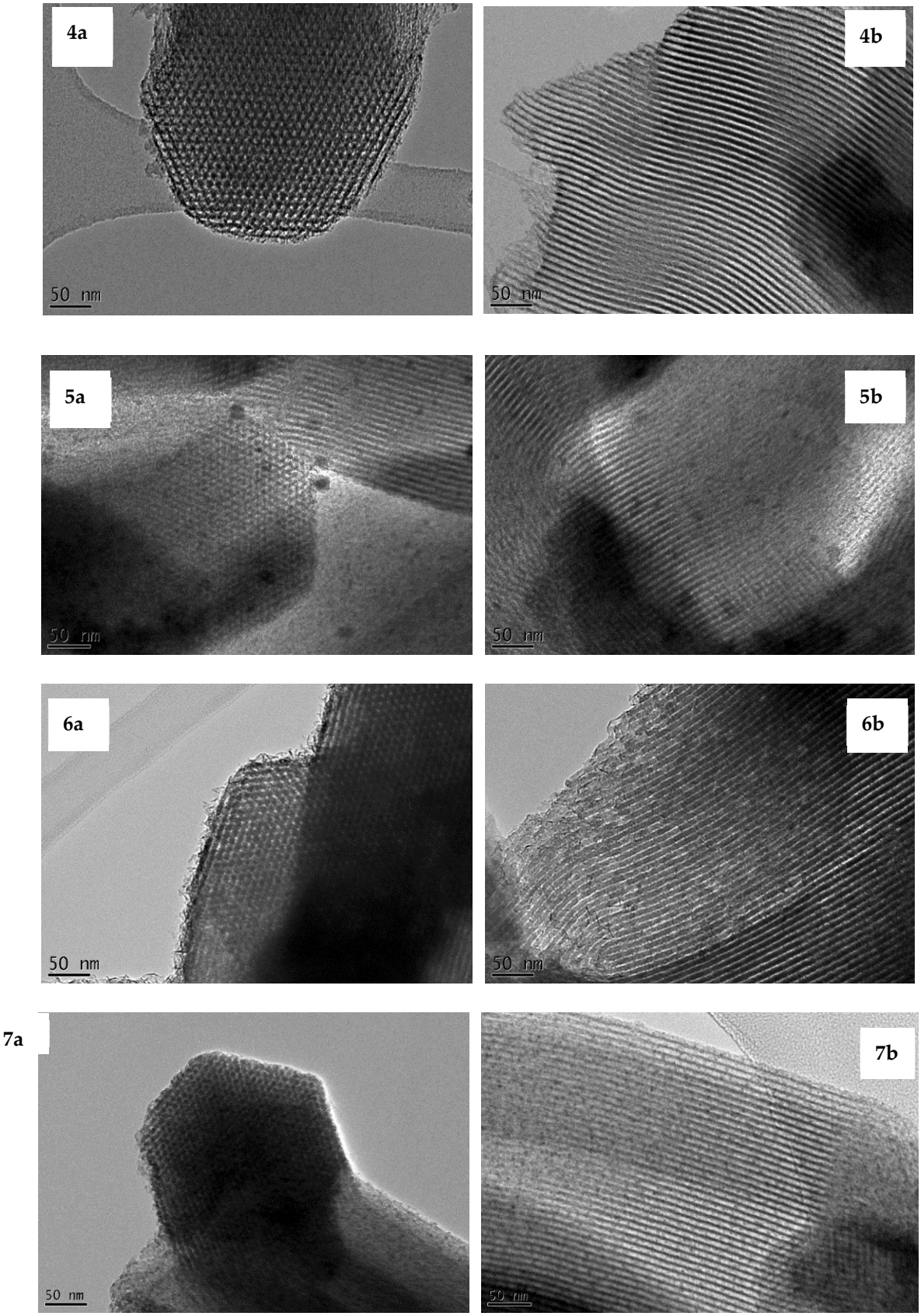

Figure 2. TEM images of pure SBA-15 support (A&B), Ni/SBA-15 - H_2O at 90 °C, unwashed (1a - b), Ni/SBA-15-H_2O at RT, unwashed (2a - b), Ni/SBA-15 – En unwashed (3a - b), Ni/SBA-15 – En washed (4a - b), Ni/SBA-15 – NH_4OH unwashed (5a - b), Ni/SBA-15 – NH_4OH washed (6a – b) and Ni/SBA-15 EDTA unwashed (7a – b).

 doi:10.20944/preprints202502.2123.v1

3.3. Wide-Angle X-Ray Diffraction (XRD)

Wide-angle XRD was used to analyse the presence and size of nickel oxide particles present on SBA-15. The results agree with TEM as samples unwashed had bigger NiO particles compared to washed samples.

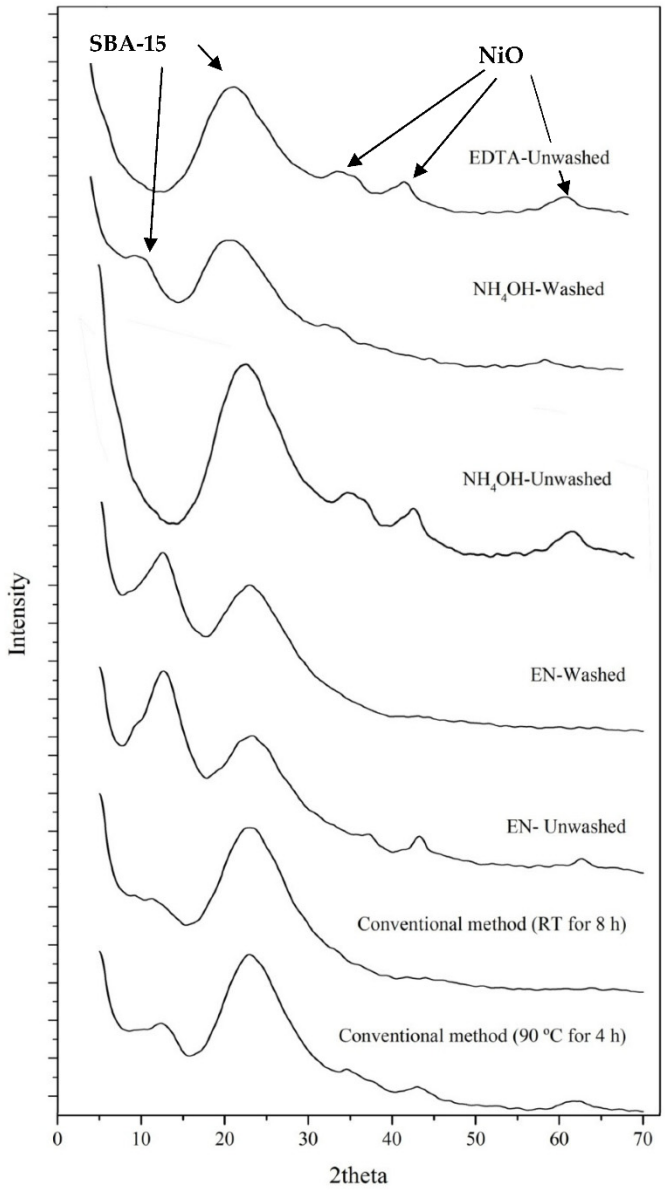

Figure 3. Wide-angle XRD of the seven Ni/SBA-15 catalysts to confirm the presence and sizes of NiO particles on the support.

Table 1. Average nickel particles size based on TEM and Wide-angle XRD.

No.	Ni/SBA-15 catalysts	Average nickel particle size – TEM and Wide angle XRD
1.	Conventional at 90 °C, unwashed	3nm and below
2.	Conventional at RT, unwashed	20 – 50 nm (TEM only)
3.	En unwashed	4 – 8 nm
4.	En washed	Less than 1nm

 doi:10.20944/preprints202502.2123.v1

5.	NH_4OH unwashed	3nm
6.	NH_4OH washed	Less than 1nm
7.	EDTA	3nm

3.4. Physical Properties of the Catalysts

In general, as shown in Table 2, all the catalysts have high surface areas, large pore volume and sizes with only Ni/SBA-15 (H_2O at RT, unwashed) catalyst having lowest Ni loading of 3 w/w %. Ni/SBA-15 (H_2O at 90 °C, unwashed) catalyst has the largest pore volume. Ni/SBA-15 (EDTA unwashed) and Ni/SBA-15 (NH_4OH washed) have the highest surface areas of 588 and 539 m^2/g respectively. Ni/SBA-15 (H_2O at 90 °C, unwashed) and Ni/SBA-15 (NH_4OH unwashed) catalysts have the highest Ni loading of 6.2 and 6.1 w/w % respectively. Unlike Ni/SBA-15 (H_2O) as-synthesised samples, Ni/SBA-15 catalysts prepared using nickel ethylenediamine and ammonium hydroxide lost small amount of Ni after washing with water, an indication that only strongly attached nickel remained on SBA-15 support for these catalysts after washing as-synthesised samples with water.

Table 2. Physical properties of support and different Ni/ SBA-15 catalyst samples.

No.	Support/ Ni/SBA-15 catalyst	BET surface area (m^2/g)	Pore volume (cm^3/g)	Pore size (nm)	Ni loading (w/w %)
	SBA-15	794	0.86	5.4	-
1.	Conventional at 90 °C, unwashed	485	0.82	6.6	6.2
2.	Conventional at RT, unwashed	482	0.64	6.5	3.0
3.	En unwashed	478	0.69	6.4	5.4
4.	En washed	491	0.77	6.8	4.6
5.	NH_4OH unwashed	496	0.55	5.0	6.1
6.	NH_4OH washed	539	0.65	5.3	5.7
7.	EDTA	588	0.71	6.1	4.8

3.5. Hydrogen Temperature Programmed Reduction (TPR)

Hydrogen reduction intensity is recorded as troughs in CATLAB-MS graphs. NiO is reduced from Ni^{2+} to Ni^0. Depending on the NiO particle strength of attachment to the support, hydrogen reduction can occur at the lower temperature range (~370 – 570 °C) or at the higher temperature range (600 – 900 °C). When hydrogen reduction occur at the lower temperature range, it means the catalyst has weakly attached nickel particles on the support; while reduction at higher temperature range confirm strongly attached nickel particles on the support. When a catalyst has hydrogen reduction occurring within the low and high temperature ranges, having more than one trough, it indicates that both weak and strongly attached nickel particles are present [56,57].

TPR result for Ni/SBA-15 (H_2O at 90 °C, unwashed) catalyst (Figure 4, 1) had TPR showed reduction at 200, 450 and 575 °C respectively, an indication of both weak and strong nickel attachment to SBA-15. Some amount of hydrogen was released around 740 °C which appears as a peak, suspect to be undecomposed nickel complex. To investigate this observation, the as-synthesised Ni/SBA-15 (H_2O at 90 °C, unwashed) sample was calcined at 700 °C in air to completely burn off the complex. TPR of the new sample calcined at 700 °C was quite different from the initial sample as peak at 740 °C disappeared. Some reduction occured between 200 – 300 °C and the major reduction trough

 doi:10.20944/preprints202502.2123.v1

appeared at 720 °C. This result suggests that higher calcination temperature was required for this catalyst to completely burn off the complex to generate more stronger attachment of nickel particles to SBA-15 support. For Ni/SBA-15 (EDTA unwashed) catalyst, a peak intensity was also observed, this time at 650 °C for undecomposed complex which realsed hydrogen. This increase in hydrogen appeared as a peak signal. Calcination at 700 °C removed the complex, however, it had minimal improvement on nickel-SBA-15 attachment, with some reduction occurring at 650 °C, and others at the other lower temperature range of 300 and 475 °C respectively. The case is different for washed Ni/SBA-15 samples prepared using ethylendiamine and ammonium hydroxide. Ni/SBA-15 (En washed) catalyst was slightly reducible at 600 and 800 °C, while Ni/SBA-15 (NH_4OH washed) catalyst had most reduction at higher temperature range of , 675 °C and a little reduction trough was observed at 450 °C which may suggest that although few detached nickel particles were still present, most nickel particles were strongly attached to SBA-15.

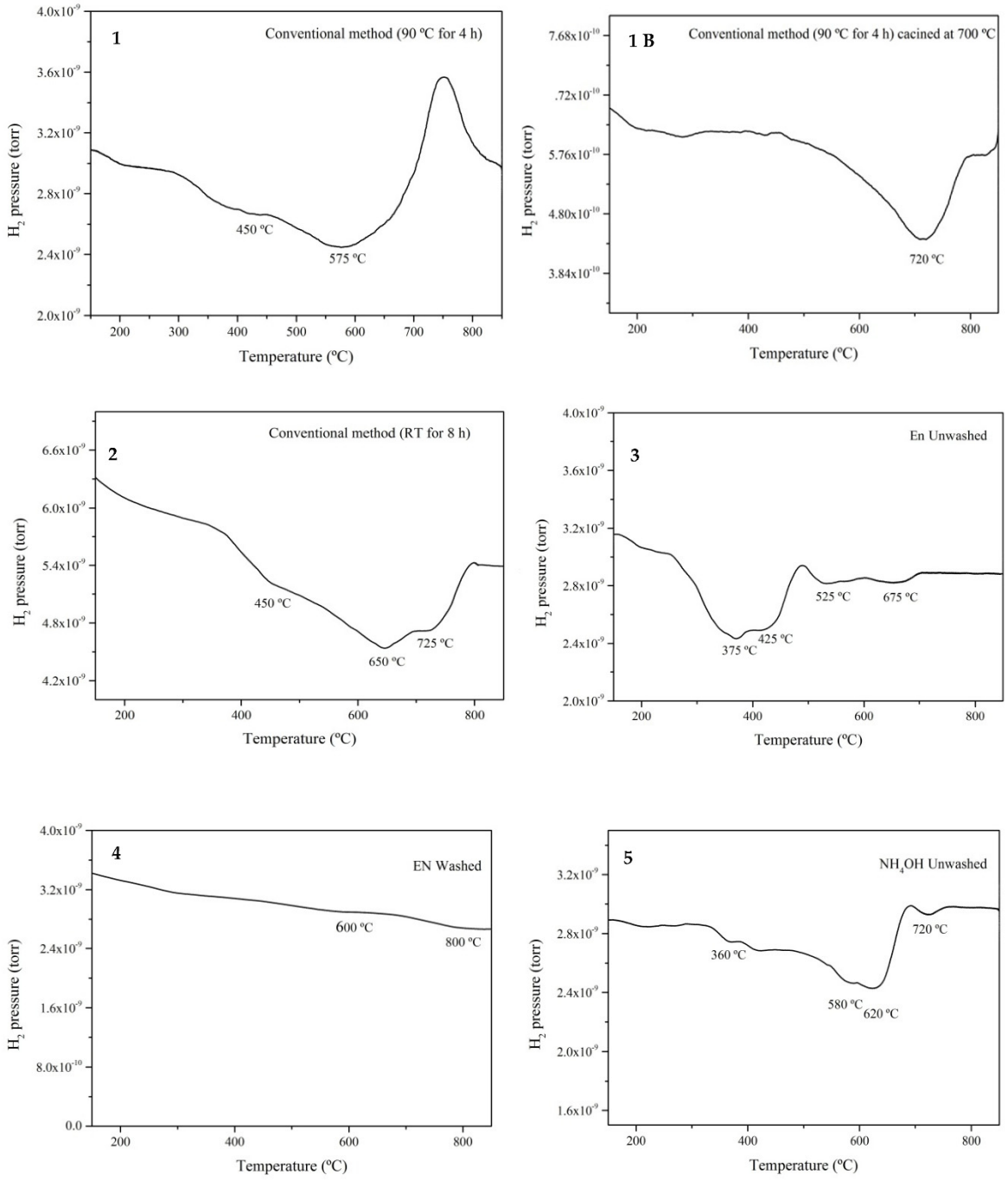

 doi:10.20944/preprints202502.2123.v1

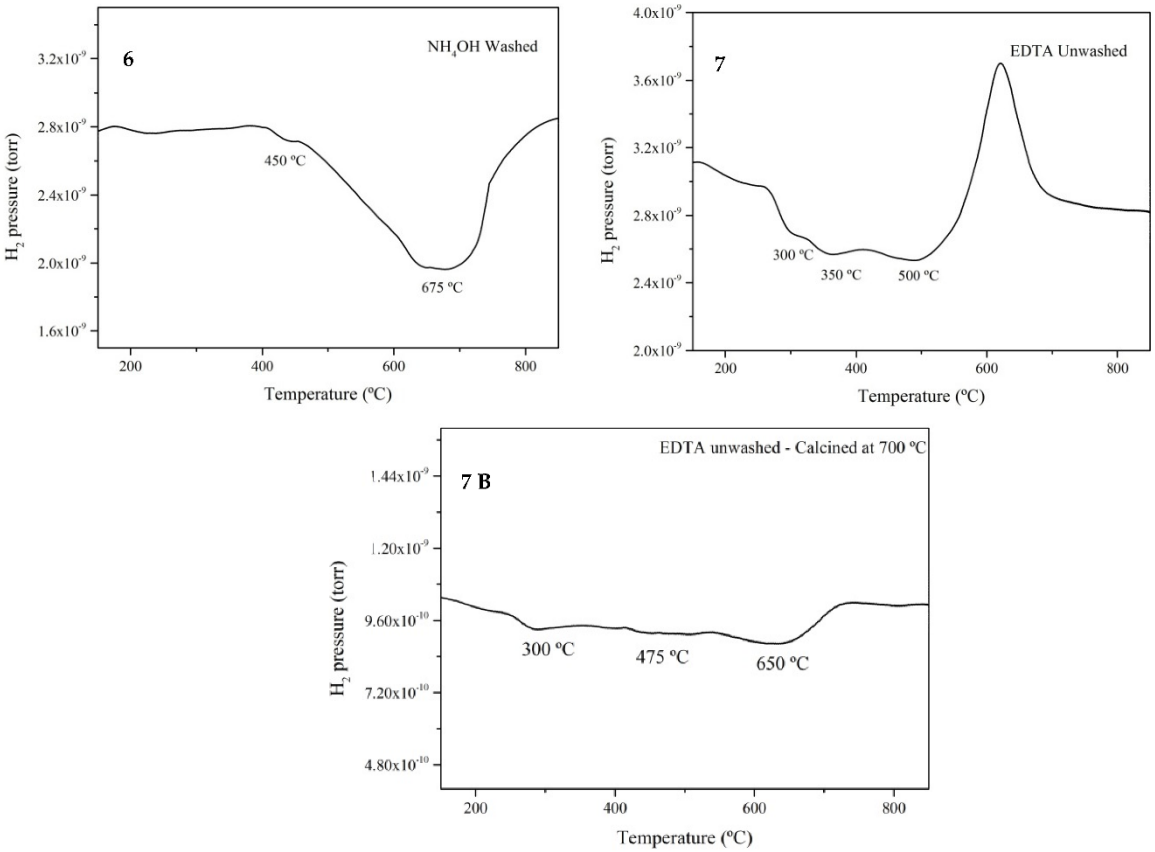

Figure 4. TPR of Ni/SBA-15 - H_2O at 90 °C, unwashed (1), Ni/SBA-15-H_2O at 90 °C, unwashed calcined at 700 °C (1B), Ni/SBA-15-H_2O at RT, unwashed (2), Ni/SBA-15 – En unwashed (3), Ni/SBA-15 – En washed (4), Ni/SBA-15 – NH_4OH unwashed (5), Ni/SBA-15 – NH_4OH washed (6), Ni/SBA-15 – EDTA unwashed (7), Ni/SBA-15 – EDTA unwashed calcined at 700 °C (7B).

3.6. Temperature Programmed Reaction (TPRx) – Catalyst Activity

TPRx from room temperature to 850 °C at 20 °/min was carried out to quickly test the catalytic performance of all the prepared Ni/SBA-15 catalysts. The results (Figure 5) show that all the catalysts were highly active in DRM, producing only hydrogen and carbon monoxide, with start of reaction temperature occurring between 250 – 300 °C, except for Ni/SBA-15 (EDTA unwashed) catalyst with start off temperature at 460 °C with corresponding decrease in CH_4 and CO_2 partial pressures in all cases. CO_2 was nearly consumed completely since it is the limiting- reactant.

 doi:10.20944/preprints202502.2123.v1

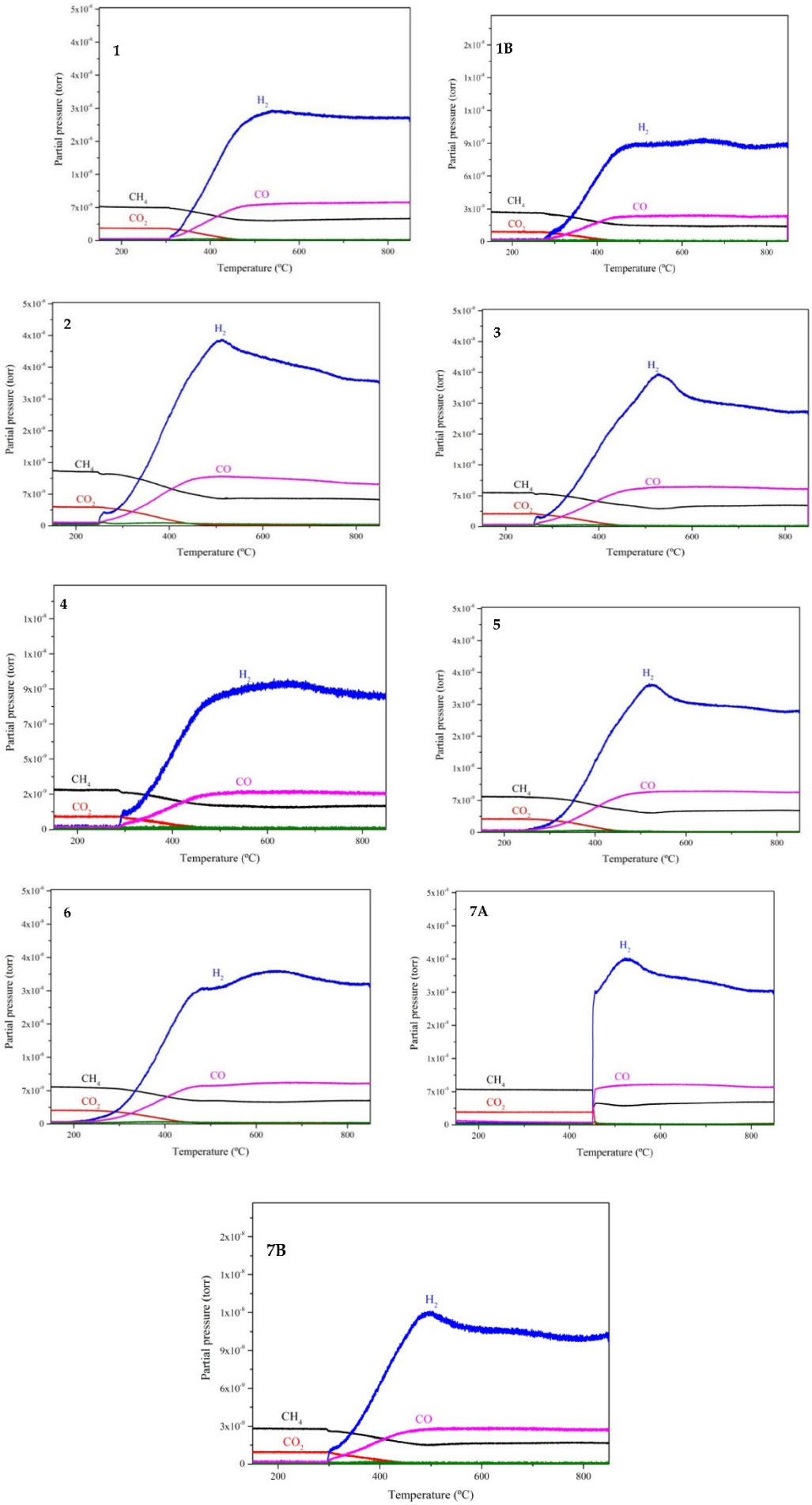

 doi:10.20944/preprints202502.2123.v1

Figure 5. TPRx of Ni/SBA-15 - H_2O at 90 °C, unwashed (1), Ni/SBA-15-H_2O at 90 °C, unwashed calcined at 700 °C (1B), Ni/SBA-15 H_2O at RT, unwashed (2), Ni/SBA-15 – En unwashed (3), Ni/SBA-15 – En washed (4), Ni/SBA-15 – NH_4OH unwashed (5), Ni/SBA-15 – NH_4OH washed (6), Ni/SBA-15 – EDTA unwashed (7), Ni/SBA-15 – EDTA unwashed calcined at 700 ºC (7B).

3.7. TPRx - Catalyst Stability

The activity and stability of the nine Ni/SBA-15 catalysts were tested in continuous flow of 2.7: 1 CH_4/CO_2 ratio at 800 °C for 360 minutes to measure the ability of the catalysts to resist coking . After 6 hrs time on stream, Ni/SBA-15 (EDTA-U), Ni/SBA-15 EDTA-U @700 °C and Ni/SBA-15 (H_2O, RT) catalysts showed some sign of gradual deactivation as CO_2 conversion decreased with time (Figure 6). The rest of the catalyst remained stable throughout time on stream reaction. The high methane conversions for all the catalysts (Figure 7) includes in addition to DRM, some extra methane decomposition that took place due to higher CH_4/CO_2 ratio. Ni/SBA-15 (EDTA-U) catalyst calcined at 700 ºC has the highest methane conversion of 63%. Due to the high decomposition of methane at 800 ºC for the catalysts, it is expected that high carbon formation will occur rapidly and only the most coke resistant catalyst will maintain high activity with little coking in such reaction condition. TGA analysis was done on the spent catalysts to compare the level of carbon depositions as a way of predicting the catalyst resistance to coking.

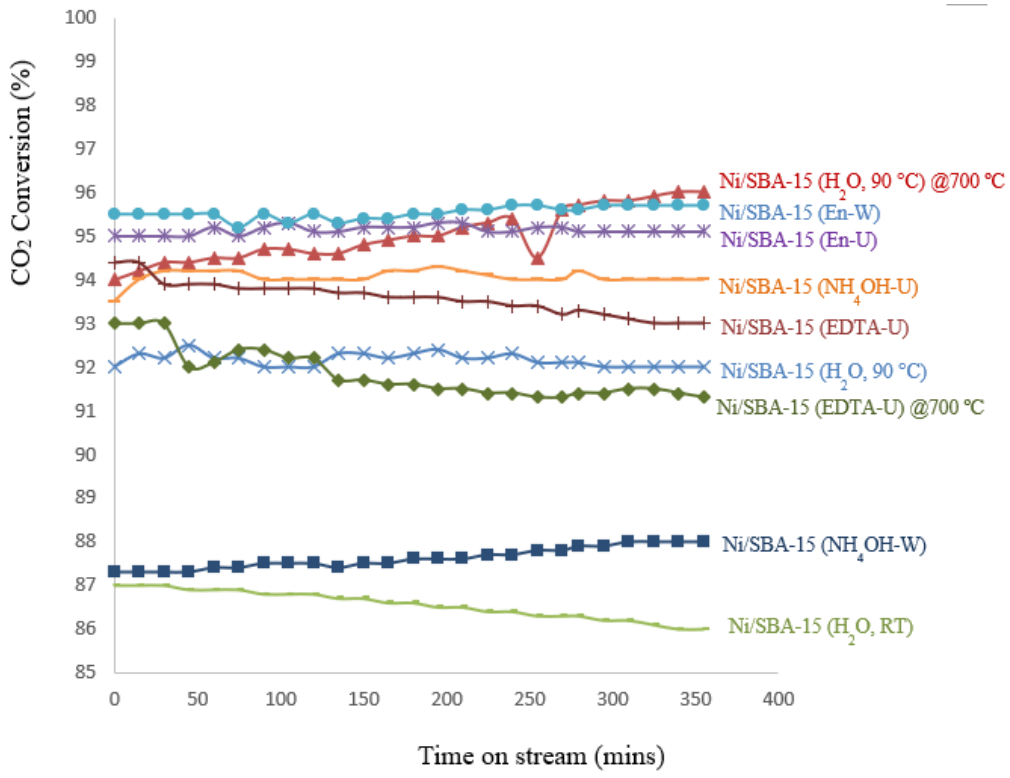

Figure 6. CO_2 conversion vs time on stream for the nine Ni/SBA-15 catalysts at 800 °C.

Preprints.org (www.preprints.org) | NOT PEER-REVIEWED | Posted: 27 February 2025 doi:10.20944/preprints202502.2123.v1

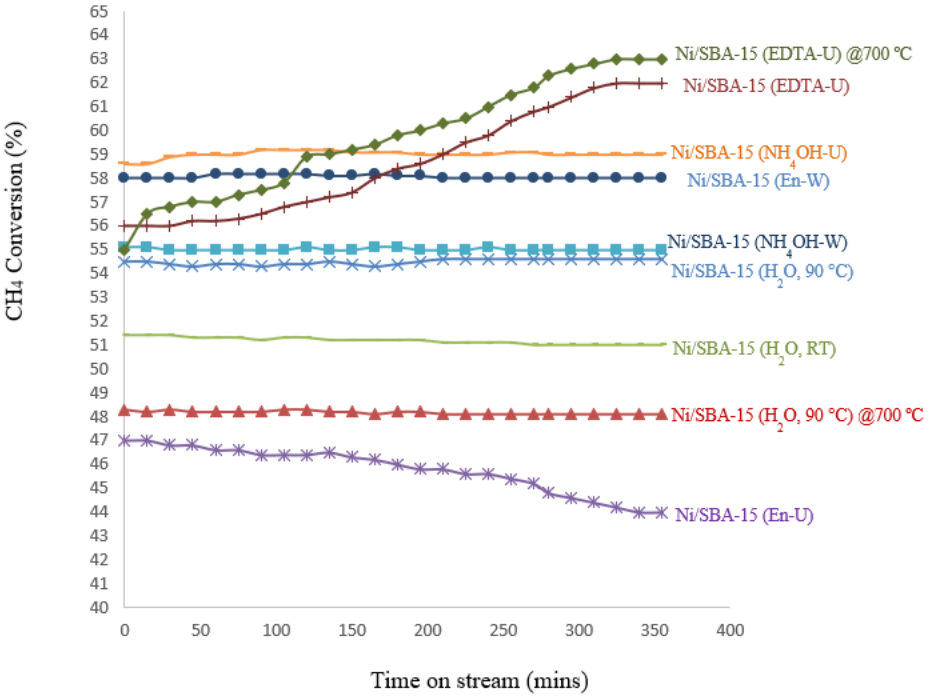

Figure 7. CH_4 conversion vs time on stream for the nine Ni/SBA-15 catalysts at 800 °C.

3.8. Carbon Deposition Analysis

The weight loss of spent catalysts were carried out in oxidative atmosphere with TGA heated from room temperature to 1000 °C. Weight loss below 160 °C is attributed to loss of adsorbed moisture on the catalysts. For all the catalysts, hydrogen reduced nickel particles were oxidized back to NiO between 250 – 390 °C. Two type of carbon species were detected. Filamentous carbon which is burnt off between 400 – 800 and graphite carbon 800 – 1000 °C [58]. Amorphous type of carbon which is the easiest type of carbon to be oxidized around 300 °C was not detected in any of the catalyst, an indication that all the catalysts where capable of eliminating amorphous carbon during DRM, however, TGA analysis reveal that all the unwashed as-synthesied catalysts before calcination had filamentous carbon deposition with Ni/SBA-15 (H_2O, RT) catalyst having the highest amount at 1.75%, this is in agreement with TEM results which confirmed that the same catalyst had the poorest nickel dispersion on SBA-15 and consequently, most prone to coking due to unattached nickel particles. TEM results also revealed that Ni/SBA-15 catalysts from En and NH_4OH unwashed as-synthesised catalysts before calcination had loosely attached nickel particles. This explains why the finished catalysts recorded the formation of 0.97 and 0.55% filamentous carbon respectively, even though the complex had strong attraction to SBA-15 support. The case was completely different with washed as-synthesied samples from En and NH_4OH as they recorded no formation of filamentous carbon. The TGA results confirm that having small nickel particles with strong metal-support attachment in addition to washing off any loosly attached nickel particle on the support can completely eliminate the formation of filamentous carbon on the surface of catalysts during DRM thereby prolonging catalyst activity and life time. This is where the novelty behind the newly decribed catalyst preparation method lies. Only the Ni/SBA-15 washed with water had the least graphite carbon and overall, insignificantly low amount of carbon deposition as shown in Table 3.

Table 3. Thermal Gravimetric Analysis (TGA) of spent catalysts.

Ni/SBA-15 Catalyst	% Filamentous carbon (400 – 800 ºC)	% Graphite carbon (800 - 1000 ºC)	Total carbon deposition (%)
Ni/SBA-15 - H_2O at 90 °C	-	0.47	0.47
Ni/SBA-15 - H_2O at 90 °C calcined at 700 ºC	0.13	0.27	0.40

 doi:10.20944/preprints202502.2123.v1

Ni/SBA-15 - H_2O at 90 °C	1.75	0.23	1.98
En-Unwashed	0.97	0.26	1.23
En-Washed	-	0.13	0.13
NH_4OH-Unwashed	0.55	0.27	0.57
NH_4OH-Washed	-	0.08	0.08
EDTA-Unwashed	0.64	0.10	0.74
EDTA-Unwashed calcined at 700 ºC	1.19	0.32	1.51

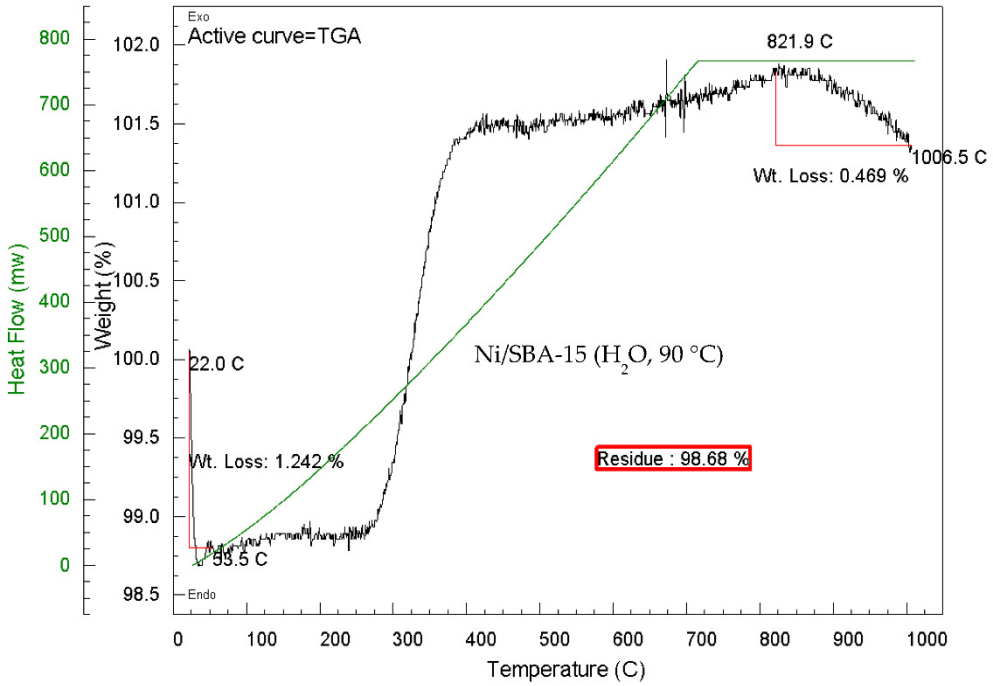

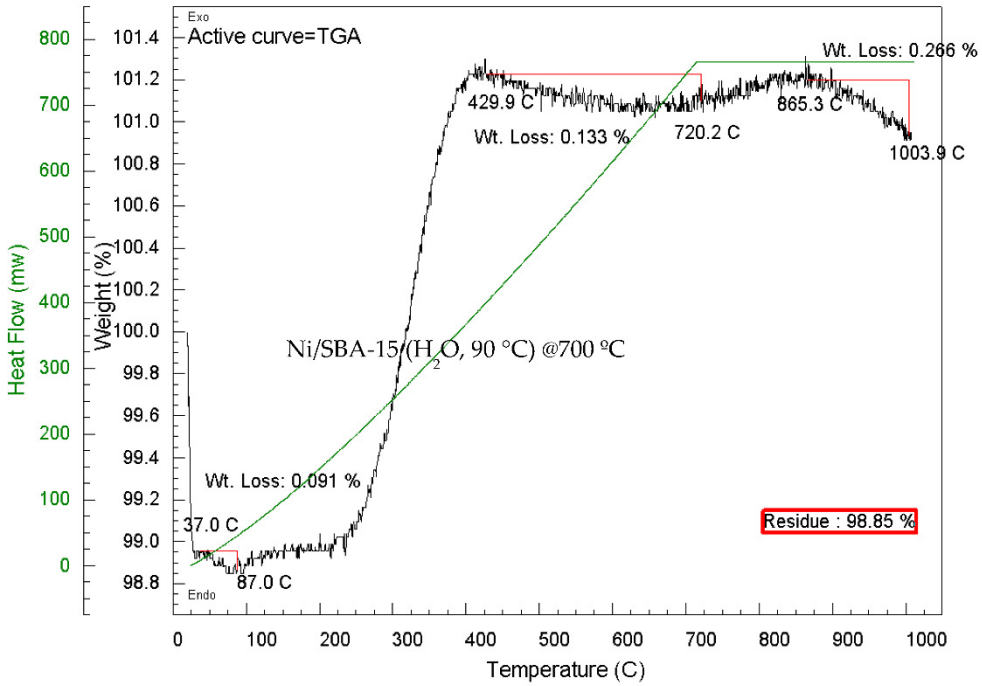

 doi:10.20944/preprints202502.2123.v1

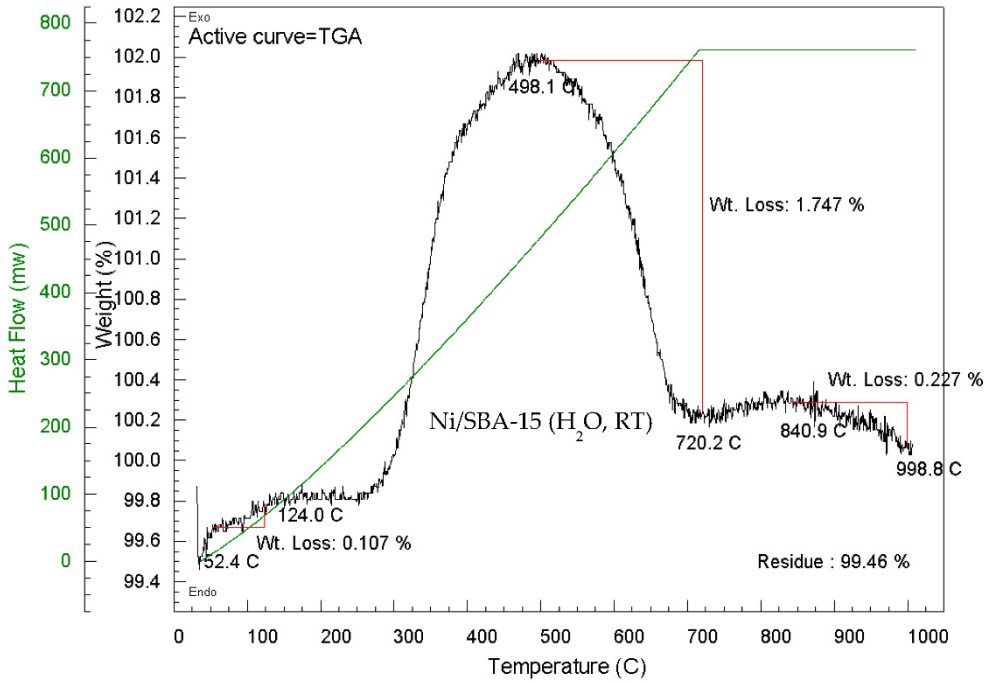

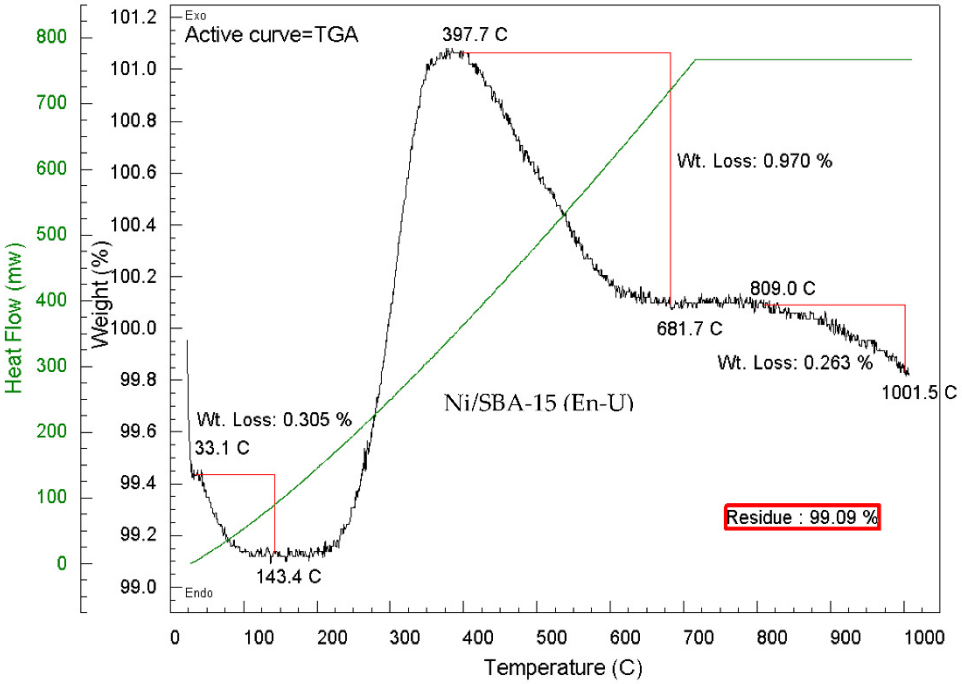

 doi:10.20944/preprints202502.2123.v1

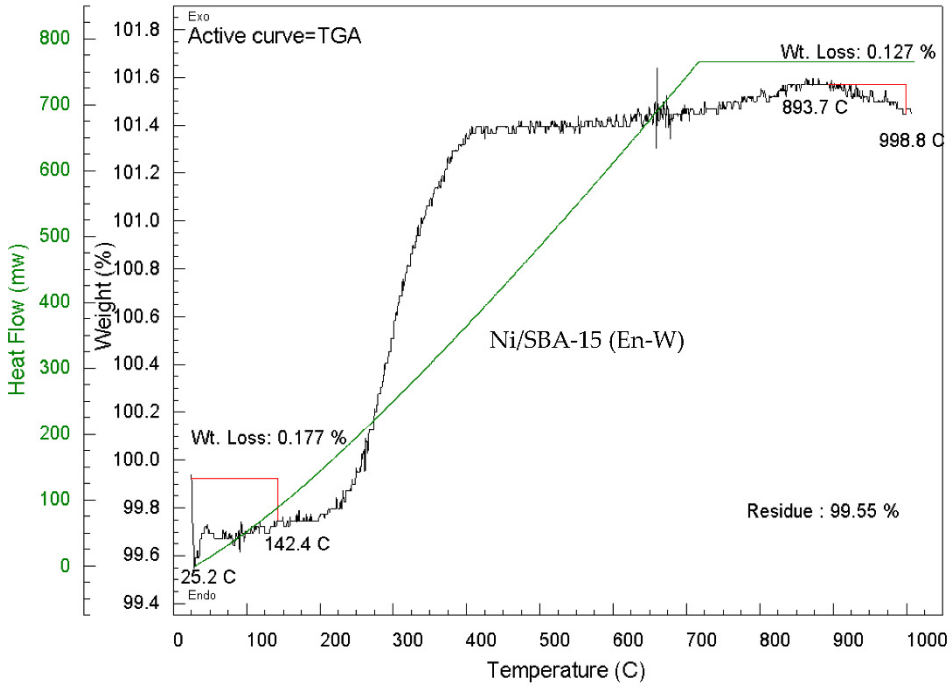

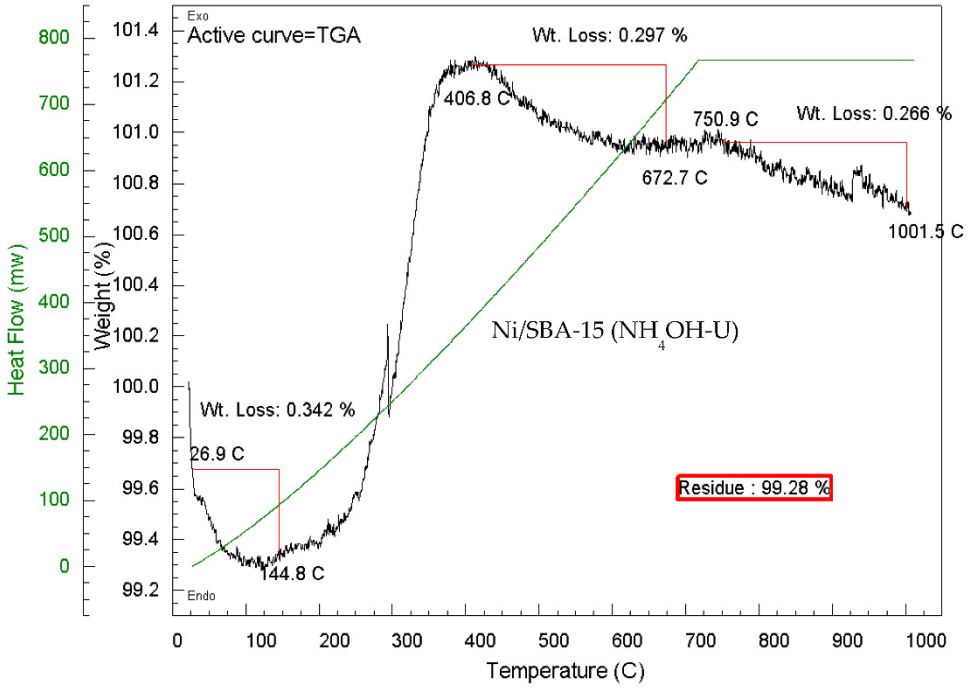

 doi:10.20944/preprints202502.2123.v1

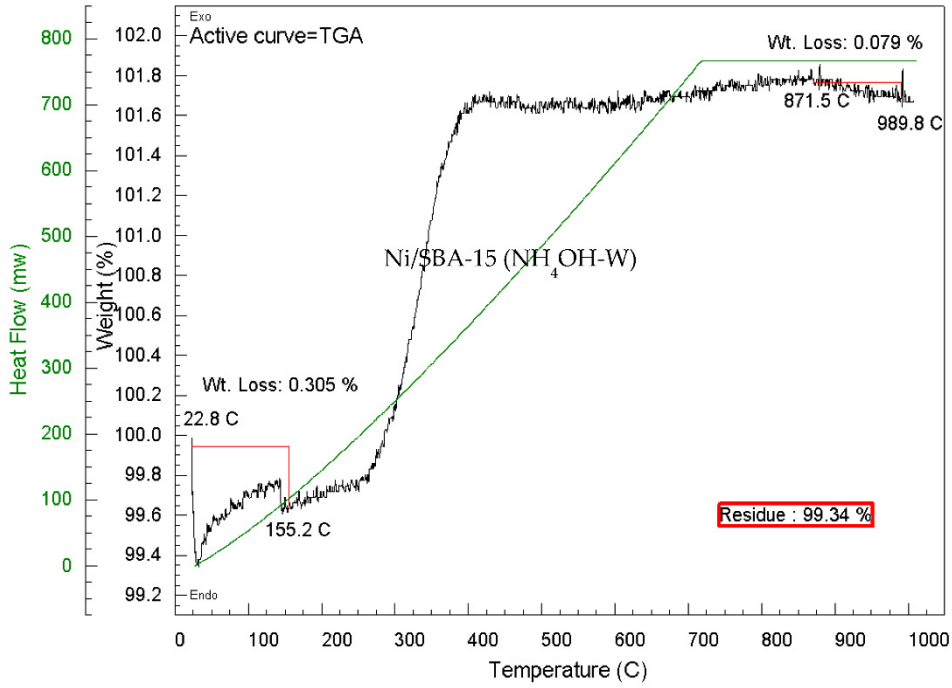

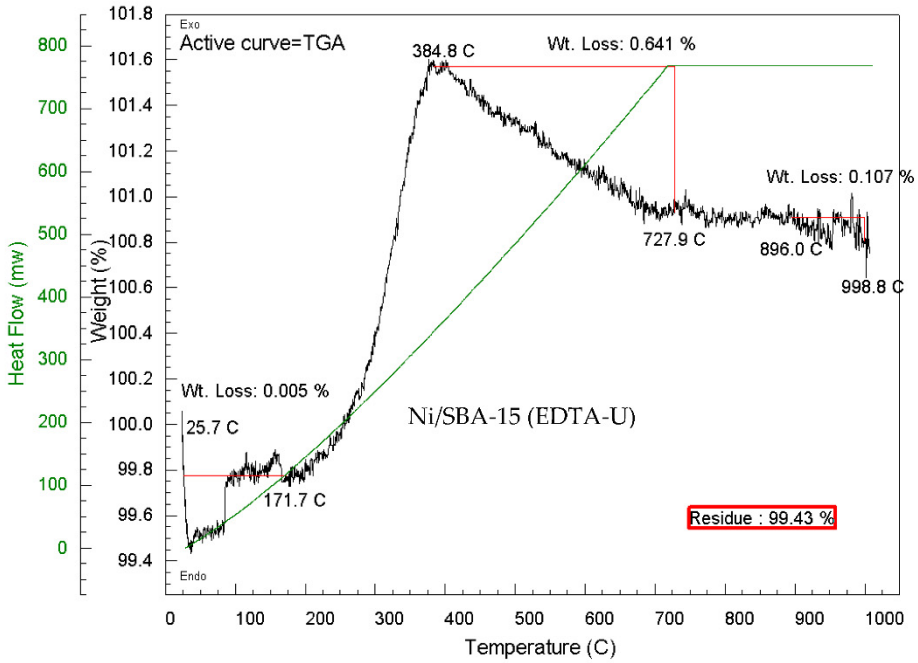

 doi:10.20944/preprints202502.2123.v1

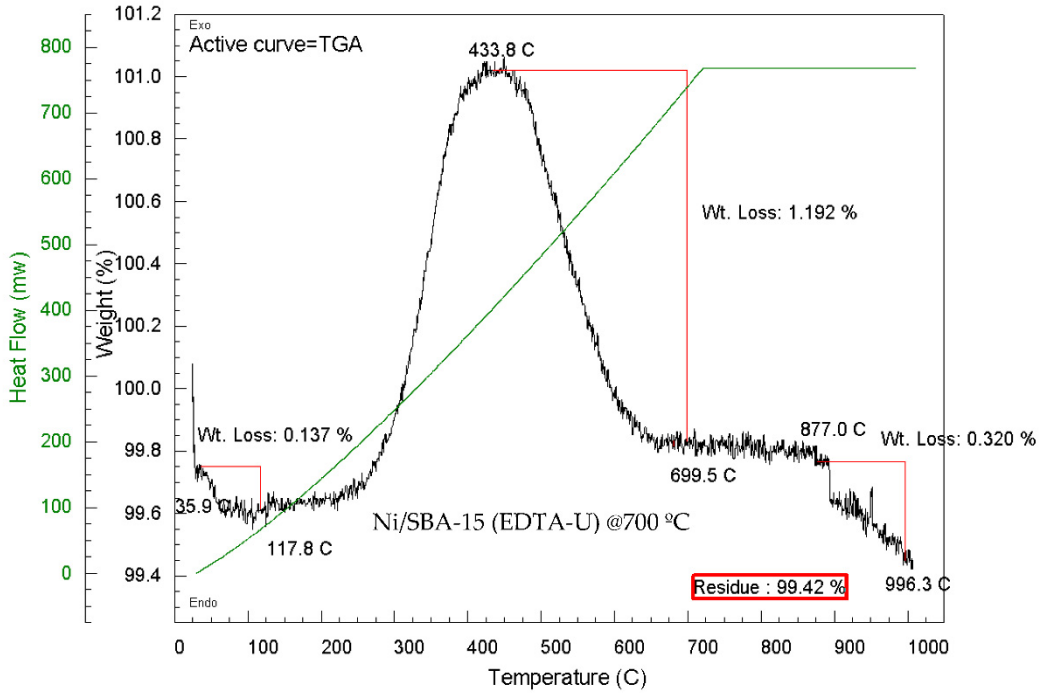

Figure 8. TGA graphs of all the spent Ni/SBA-15 catalysts.

4. Conclusion

This research has demonstrated that it is possible to develop nickel based catalysts with high activity, stability and resistance to coking in dry (CO_2) reforming of methane. Novel preparation methods with $[Ni(NH_3)_6]^{2+}$ and $[Ni(En)_3]^{2+}$ complexes promoted a stronger attachment between nickel and SBA-15 support which generated ultrafine nickel paricles on SBA-15. However, the dependance of strong interaction between the nickel complex on the catalyst support alone is not sufficient to resist carbon deposition. There is in addition, the need to wash off loosely bond nickel particles from the asynthesied catalyst to mitigate against carbon build up on bigger nickel particles during DRM reaction.By washing the as-synthesised catalysts with water, some loosely attached nickel particles which are always present and easily prone to coking were washed off the catalyst surface, leaving mostly strongly attached ultrafine nickel particles on the support. Also, the use of hydrothermally stable SBA-15 mesoporous silica with high specific surface area, large pore size and volume as catalyst support contributed significantly to catalyst high activity and stability in high temperature DRM reaction for all the catalysts. Silica as catalyst support for dry reforming of methane was previously reported as easily prone to carbon deposition [39], our investigation reveals however, that the main problem lie in the development of a suitable preparation method capable of generating uniformly dispersed ultrafine nickel particles on hydrothermally stable mesoporous silica with high surface area, and eliminating the loosly attached nickel particles by washing to inhibit carbon deposition and prevent catalyst deactivation [59,60]

This novel preparation method can potentially remove the major hinderance to the commercial scaling-up of nickel based catalysts for dry reforming of methane, even in cases with higher CH_4/CO ratio used. It is expected that this prelimainary body of work will encourage more research into the use of specific nickel complexes and washing the asynthesised catalyst to generate strongly attached, ultrafine nickel particles on catalyst support materials which was shown to promote coke resistant nickel based catalysts in dry reforming of methane reactions.

 doi:10.20944/preprints202502.2123.v1

References

1. Solymosi, F.; Kutsán, G.; Erdöhelyi, A. Catalytic reaction of CH_4 with CO_2 over alumina-supported Pt metals. *Catal. Lett.* **1991**, *11*, 149–156.
2. Zhang, Z.L.; Tsipouriari, V.A.; Efstathiou, A.M.; Verykios, X.E. Reforming of methane with carbon dioxide to synthesis gas over supported rhodium catalysts: I. Effects of support and metal crystallite size on reaction activity and deactivation characteristics. *J. Catal.* **1996**, *158*, 51–63.
3. Valderrama, G.; Goldwasser, M.R.; Navarro, C.U.d.; Tatibouët, J.M.; Barrault, J.; Batiot-Dupeyrat, C.; Martínez, F. Dry reforming of methane over Ni perovskite type oxides. *Catal. Today* **2005**, *107–108*, 785–791.
4. Bradford, M.; Vannice, M. CO_2 reforming of CH_4. *Catal. Rev.* **1999**, *41*, 1–42.
5. Edwards, J.H. Potential sources of CO_2 and the options for its large-scale utilisation now and in the future. *Catal. Today* **1995**, *23*, 59–66.
6. Tsang, S.C.; Claridge, J.B.; Green, M.L.H. Recent advances in the conversion of methane to synthesis gas. *Catal. Today* **1995**, *23*, 3–15.
7. Teuner, S. MAKE CO FROM CO_2. *Hydrocarbon Process.* **1985**, *64*, 106–107.
8. Maroto-Valer, M.M.; Song, C.; Soong, Y. Environmental challenges and greenhouse gas control for fossil fuel utilization in the 21st century. Springer Science & Business Media, 2012.
9. Demirel, B.; Scherer, P. The roles of acetotrophic and hydrogenotrophic methanogens during anaerobic conversion of biomass to methane: a review. *Rev. Environ. Sci. Biotechnol.* **2008**, *7*, 173–190.
10. Gunaseelan, V.N. Anaerobic digestion of biomass for methane production: A review. *Biomass Bioenergy* **1997**, *13*, 83–114.
11. McKendry, P. Energy production from biomass (part 2): conversion technologies. *Bioresour. Technol.* **2002**, *83*, 47–54.
12. Demirbaş, A. Biomass resource facilities and biomass conversion processing for fuels and chemicals. *Energy Convers. Manag.* **2001**, *42*, 1357–1378.
13. Balat, M.; Balat, M.; Kırtay, E.; Balat, H. Main routes for the thermo-conversion of biomass into fuels and chemicals. Part 2: Gasification systems. *Energy Convers. Manag.* **2009**, *50*, 3158–3168.
14. Bereketidou, O.A.; Goula, M.A. Biogas reforming for syngas production over nickel supported on ceria–alumina catalysts. *Catal. Today* **2012**, *195*, 93–100.
15. Centi, G.; Quadrelli, E.A.; Perathoner, S. Catalysis for CO_2 conversion: a key technology for rapid introduction of renewable energy in the value chain of chemical industries. *Energy Environ. Sci.* **2013**, *6*, 1711–1731.
16. Wang, S.; Lu, G.Q.; Millar, G.J. Carbon Dioxide Reforming of Methane To Produce Synthesis Gas over Metal-Supported Catalysts: State of the Art. *Energy Fuels* **1996**, *10*, 896–904.
17. Fukuhara, C.; Hyodo, R.; Yamamoto, K.; Masuda, K.; Watanabe, R. A novel nickel-based catalyst for methane dry reforming: A metal honeycomb-type catalyst prepared by sol–gel method and electroless plating. *Appl. Catal. A Gen.* **2013**, *468*, 18–25.
18. Erdohelyi, A.; Cserenyi, J.; Solymosi, F. Activation of CH4 and Its Reaction with CO_2 over Supported Rh Catalysts. *J. Catal.* **1993**, *141*, 287–299.
19. Guo, J.; Lou, H.; Zhao, H.; Chai, D.; Zheng, X. Dry reforming of methane over nickel catalysts supported on magnesium aluminate spinels. *Appl. Catal. A Gen.* **2004**, *273*, 75–82.
20. Hou, Z.; Chen, P.; Fang, H.; Zheng, X.; Yashima, T. Production of synthesis gas via methane reforming with CO2 on noble metals and small amount of noble-(Rh-) promoted Ni catalysts. *Int. J. Hydrogen Energy* **2006**, *31*, 555–561.
21. Richardson, J.T.; Paripatyadar, S.A. Carbon dioxide reforming of methane with supported rhodium. *Appl. Catal.* **1990**, *61*, 293–309.
22. Verykios, X.E. Catalytic dry reforming of natural gas for the production of chemicals and hydrogen. *Int. J. Hydrogen Energy* **2003**, *28*, 1045–1063.
23. Kambolis, A.; Matralis, H.; Trovarelli, A.; Papadopoulou, C. Ni/CeO_2-ZrO_2 catalysts for the dry reforming of methane. *Appl. Catal. A Gen.* **2010**, *377*, 16–26.
24. Bartholomew, C.H. Mechanisms of catalyst deactivation. *Appl. Catal. A Gen.* **2001**, *212*, 17–60.

 doi:10.20944/preprints202502.2123.v1

25. Liu, D.; Quek, X.Y.; Cheo, W.N.E.; Lau, R.; Borgna, A.; Yang, Y. MCM-41 supported nickel-based bimetallic catalysts with superior stability during carbon dioxide reforming of methane: Effect of strong metal–support interaction. *J. Catal.* **2009**, *266*, 380–390.
26. Wang, N.; Chu, W.; Zhang, T.; Zhao, X.S. Synthesis, characterization and catalytic performances of Ce-SBA-15 supported nickel catalysts for methane dry reforming to hydrogen and syngas. *Int. J. Hydrogen Energy* **2012**, *37*, 19–30.
27. Barroso-Quiroga, M.M.; Castro-Luna, A.E. Catalytic activity and effect of modifiers on Ni-based catalysts for the dry reforming of methane. *Int. J. Hydrogen Energy* **2010**, *35*, 6052–6056.
28. Hou, Z.; Yashima, T. Small amounts of Rh-promoted Ni catalysts for methane reforming with CO_2. *Catal. Lett.* **2003**, *89*, 193–197.
29. Therdthianwong, S.; Siangchin, C.; Therdthianwong, A. Improvement of coke resistance of Ni/Al2O3 catalyst in CH_4/CO_2 reforming by ZrO_2 addition. *Fuel Process. Technol.* **2008**, *89*, 160–168.
30. Lemonidou, A.A.; Vasalos, I.A. Carbon dioxide reforming of methane over 5 wt.% Ni/CaO-Al_2O_3 catalyst. *Appl. Catal. A Gen.* **2002**, *228*, 227–235.
31. Corthals, S.; Van Nederkassel, J.; Geboers, J.; De Winne, H.; Van Noyen, J.; Moens, B.; Sels, B.; Jacobs, P. Influence of composition of $MgAl_2O_4$ supported $NiCeO_2ZrO_2$ catalysts on coke formation and catalyst stability for dry reforming of methane. *Catal. Today* **2008**, *138*, 28–32.
32. Zhu, Y.-A.; Chen, D.; Zhou, X.-G.; Yuan, W.-K. DFT studies of dry reforming of methane on Ni catalyst. *Catal. Today* **2009**, *148*, 260–267.
33. Ginsburg, J.M.; Piña, J.; El Solh, T.; de Lasa, H.I. Coke Formation over a Nickel Catalyst under Methane Dry Reforming Conditions: Thermodynamic and Kinetic Models. *Ind. Eng. Chem. Res.* **2005**, *44*, 4846–4854.
34. Gadalla, A.M.; Bower, B. The role of catalyst support on the activity of nickel for reforming methane with CO_2. *Chem. Eng. Sci.* **1988**, *43*, 3049–3062.
35. Rostrup-Nielsen, J.; Trimm, D.L. Mechanisms of carbon formation on nickel-containing catalysts. *J. Catal.* **1977**, *48*, 155–165.
36. Rostrupnielsen, J.R.; Hansen, J.H.B. CO_2-Reforming of Methane over Transition Metals. *J. Catal.* **1993**, *144*, 38–49.
37. Chen, D.; Lødeng, R.; Anundskås, A.; Olsvik, O.; Holmen, A. Deactivation during carbon dioxide reforming of methane over Ni catalyst: microkinetic analysis. *Chem. Eng. Sci.* **2001**, *56*, 1371–1379.
38. Kroll, V.C.H.; Swaan, H.M.; Mirodatos, C. Methane Reforming Reaction with Carbon Dioxide Over Ni/SiO_2 Catalyst: I. Deactivation Studies. *J. Catal.* **1996**, *161*, 409–422.
39. Tang, S.B.; Qiu, F.L.; Lu, S.J. Effect of supports on the carbon deposition of nickel catalysts for methane reforming with CO_2. *Catal. Today* **1995**, *24*, 253–255.
40. Olsbye, U.; Wurzel, T.; Mleczko, L. Kinetic and Reaction Engineering Studies of Dry Reforming of Methane over a Ni/La/Al2O3 Catalyst. *Ind. Eng. Chem. Res.* **1997**, *36*, 5180–5188.
41. Huang, T.; Huang, W.; Huang, J.; Ji, P. Methane reforming reaction with carbon dioxide over SBA-15 supported Ni–Mo bimetallic catalysts. *Fuel Process. Technol.* **2011**, *92*, 1868–1875.
42. Laosiripojana, N.; Assabumrungrat, S. Catalytic dry reforming of methane over high surface area ceria. *Appl. Catal. B Environ.* **2005**, *60*, 107–116.
43. Hayakawa, T.; Suzuki, S.; Nakamura, J.; Uchijima, T.; Hamakawa, S.; Suzuki, K.; Shishido, T.; Takehira, K. CO2 reforming of CH4 over Ni/perovskite catalysts prepared by solid phase crystallization method. *Appl. Catal. A Gen.* **1999**, *183*, 273–285.
44. Tomishige, K.; Chen, Y.G.; Fujimoto, K. Studies on carbon deposition in CO_2 reforming of CH_4 over nickel-magnesia solid solution catalysts. *J. Catal.* **1999**, *181*, 91–103.
45. Bitter, J.H.; Seshan, K.; Lercher, J.A. Deactivation and coke accumulation during CO_2/CH_4 reforming over Pt catalysts. *J. Catal.* **1999**, *183*, 336–343.
46. Beck, J.S.; Vartuli, J.C.; Roth, W.J.; Leonowicz, M.E.; Kresge, C.T.; Schmitt, K.D.; Chu, C.T.W.; Olson, D.H.; Sheppard, E.W. A new family of mesoporous molecular sieves prepared with liquid crystal templates. *J. Am. Chem. Soc.* **1992**, *114*, 10834–10843.
47. Kresge, C.T.; Leonowicz, M.E.; Roth, W.J.; Vartuli, J.C.; Beck, J.S. Ordered mesoporous molecular sieves synthesized by a liquid-crystal template mechanism. *Nature* **1992**, *359*, 710–712

 doi:10.20944/preprints202502.2123.v1

48. Corma, A. From Microporous to Mesoporous Molecular Sieve Materials and Their Use in Catalysis. *Chem. Rev.* **1997**, *97*, 2373–2420.
49. Zhao, D.; Feng, J.; Huo, Q.; Melosh, N.; Fredrickson, G.H.; Chmelka, B.F.; Stucky, G.D. Triblock Copolymer Syntheses of Mesoporous Silica with Periodic 50 to 300 Angstrom Pores. *Science* **1998**, *279*, 548–552.
50. Bore, M.T.; Pham, H.N.; Ward, T.L.; Datye, A.K. Role of Pore Curvature on the Thermal Stability of Gold Nanoparticles in Mesoporous Silica. *Chem. Commun.* **2004**, 2620–2621.
51. Sun, N.; Wen, X.; Wang, F.; Wei, W.; Sun, Y. Effect of Pore Structure on Ni Catalyst for CO_2 Reforming of CH_4. *Energy Environ. Sci.* **2010**, *3*, 366–369.
52. Zhang, M.; Ji, S.; Hu, L.; Yin, F.; Li, C.; Liu, H. Structural Characterization of Highly Stable Ni/SBA-15 Catalyst and Its Catalytic Performance for Methane Reforming with CO2. *Chin. J. Catal.* **2006**, *27*, 777–781.
53. Ungureanu, A.; Dragoi, B.; Chirieac, A.; Ciotonea, C.; Royer, S.; Duprez, D.; Mamede, A.S.; Dumitriu, E. Composition-Dependent Morphostructural Properties of Ni–Cu Oxide Nanoparticles Confined within the Channels of Ordered Mesoporous SBA-15 Silica. *ACS Appl. Mater. Interfaces* **2013**, *5*, 3010–3025.
54. D. Pakhare, J. Spivey, A review of dry (CO_2) reforming of methane over noble metal catalysts, Chem. Soc. Rev. 2014, 43 7813-7837.
55. E.O.Iro, Synthesis, characterisation and testing of Au/SBA-15 catalysts for elimination of volatile organic compounds by complete oxidation at low temperatures, PhD, Teesside University, Middlesbrough UK, 2017.
56. B. Mile, D. Stirling, M.A. Zammitt, A. Lovell, M. Webb, The location of nickel oxide and nickel in silica-supported catalysts: Two forms of "NiO" and the assignment of temperature-programmed reduction profiles, Journal of Catalysis, 114 (1988) 217-229.
57. F. Pompeo, N.N. Nichio, M.G. González, M. Montes, Characterization of Ni/SiO_2 and Ni/Li-SiO2 catalysts for methane dry reforming, Catalysis Today, 107–108 (2005) 856-862.
58. D. Liu, X.-Y. Quek, H.H.A. Wah, G. Zeng, Y. Li, Y. Yang, Carbon dioxide reforming of methane over nickel-grafted SBA-15 and MCM-41 catalysts, Catalysis Today, 148 (2009) 243-250.
59. T. Sodesawa, A. Dobashi, F. Nozaki, Catalytic reaction of methane with carbon dioxide, Reaction Kinetics and Catalysis Letters, 12 (1979) 107-111.
60. K. Tomishige, O. Yamazaki, Y. Chen, K. Yokoyama, X. Li, K. Fujimoto, Development of ultra-stable Ni catalysts for CO2 reforming of methane, Catalysis Today, 45 (1998) 35-39.